

## Supplementary material for

### **Wearable super-adsorptive fibrous equipment *in-situ* grafted with porous organic polymers for carcinogenic fumigant defense and detoxification**

*Peixin Tang<sup>a</sup>, Bolin Ji<sup>b</sup>, Gang Sun<sup>a\*</sup>*

<sup>a</sup>Department of Biological and Agricultural Engineering, University of California, Davis, 95616 CA, USA.

<sup>b</sup>College of Chemistry, Chemical Engineering and Biotechnology, Donghua University, Shanghai, 201620 PR China.

\* Corresponding author: Tel.: +1 530 752 0840; gysun@ucdavis.edu (G. Sun).

## Supplementary methods

### Synthesis of nucleophilic porous organic polymer (Nu-POP) from cyanuric chloride and melamine

Cyanuric chloride (7.5 mmol) was dissolved in 75 mL dimethyl sulfoxide (DMSO) (Solution 1). Then, Solution 1 was added dropwise into Solution 2, which was prepared by dissolving melamine (7.5 mmol) in 75 mL DMSO in a 250 mL round-bottom flask. And 1 mL of triethylamine ( $\text{Et}_3\text{N}$ ) was added into the system. During the mixing of Solutions 1 and 2, nitrogen gas was continuously purged into the reaction system for 20 min. After that, the flask was sealed with a glass stopper and gradually heated to 150 °C within 60 min. The reaction system was heated at 150 °C for 24 hours. The resultant egg-white precipitates were filtrated after cooling the system to room temperature and were thoroughly washed with excess amount of DMSO, deionized water, and methanol, and were dried under vacuum at room temperature. The yield was weighted as 79.8%.

### Synthesis of nonporous $N^2,N^{2'},N^{2''}$ -(1,3,5-triazine-2,4,6-triyl)tris(1,3,5-triazine-2,4,6-triamine) (1CCI-3M)

The molar ratio of CCl/melamine was controlled as 1/3 in this case. Melamine (7.5 mmol) and CCl (2.5 mmol) were dissolved in 75 mL DMSO separately.  $\text{Et}_3\text{N}$  (1 mL) was added in melamine/DMSO solution. The melamine and CCl were mixed dropwise in a 250 mL round-bottom flask. The reaction system was purged with  $\text{N}_2$  for 20 min before sealing the flask with a glass stopper. According to the temperature-dependent reactivity of three triazine-chlorides in CCl,<sup>S1</sup> the reaction system was firstly stirred at 0 °C for 1 hour. Then, the system was transferred to room temperature (25 °C) and stirred for an extra 2 hours. Finally, the system was heated to 80 °C and reacted for another 21 hours. The white precipitates were filtrated with filter paper and

washed with excess amount of DMSO, deionized water, and methanol. The particles were dried under vacuum at room temperature (yield = 48.5%). The resultant particles were structurally characterized with FTIR, whose major peaks are shown at 3393  $\text{cm}^{-1}$  ( $\nu_{(1^\circ\text{N-H})}$ ), 3230  $\text{cm}^{-1}$  ( $\nu_{(2^\circ\text{N-H})}$ ), 1735  $\text{cm}^{-1}$  and 1661  $\text{cm}^{-1}$  ( $\nu_{(\text{C=N})}$ ), 1536  $\text{cm}^{-1}$  and 1447  $\text{cm}^{-1}$  (triazine ring), and 770  $\text{cm}^{-1}$  ( $\omega_{(\text{triazine ring})}$ ).

### **Fumigant adsorption evaluations**

#### *Methyl bromide (MeBr)*

SAFE-Cotton (100 mg) was sealed in a 5 mL glass vial capped with PTFE/silicone septum. MeBr solution (10  $\mu\text{L} \times 2 \text{ mg mL}^{-1}$  in methanol) was injected into the vial with a gas-tight syringe. After different incubation times, 2 mL of headspace gas was pumped out with a 5 mL gas-tight syringe and injected into 1 mL of DMF containing 4-(*p*-nitrobenzyl)pyridine (NBP) (20 wt%). The NBP/DMF solution was incubated at 70 °C for 5 min in order to show a blue color by reacting with MeBr through an alkylation reaction, whose intensity is correlated to the residual concentration of MeBr in the vial. The color intensity was monitored with a UV-vis spectrophotometer at the maximum adsorption wavelength of  $\lambda_{\text{max}} = 573 \text{ nm}$ . The residual concentration of MeBr after adsorption can be calculated according to an established calibration curve (Fig. S15b).

#### *1,3-Dichloroproene (1.3-D)*

SAFE-Cotton (100 mg) was sealed in a 5 mL glass vial capped with PTFE/silicone septum. 1,3-D solution (8  $\mu\text{L} \times 5 \text{ mg mL}^{-1}$  in methanol) was injected into the vial with a gas-tight syringe. After different incubation times, 5 mL of headspace gas was pumped out with a 5 mL gas-tight syringe and injected into 1 mL of DMF containing 4-(*p*-nitrobenzyl)pyridine (NBP) (20 wt%). The NBP/DMF solution was incubated at 70 °C for 10 min in order to show a blue color by reacting with 1,3-D through an alkylation reaction, whose intensity is corresponding to the residual

concentration of 1,3-D in the vial. The color intensity was monitored with a UV-vis spectrophotometer at the maximum adsorption wavelength ( $\lambda_{max} = 562$  nm). The residual concentration of 1,3-D after adsorption was measured based on an established calibration curve (Fig. S15c).

### *Chloropicrin*

SAFE-Cotton (100 mg) was sealed in a 5 mL glass vial capped with PTFE/silicone septum. Chloropicrin solution ( $5 \mu\text{L} \times 1 \text{ mg mL}^{-1}$  in methanol) was injected into the vial with a gas-tight syringe. After different incubation times, 2 mL of headspace gas was pumped out with a 5 mL gas-tight syringe and injected into a standard cysteine solution, contained 2.5 mL monobasic sodium phosphate buffer (pH = 8.0) and 250  $\mu\text{L}$  0.5 mM cysteine. The system was incubated at room temperature for 15 min to allow the reaction between residual chloropicrin and the sulfhydryl group of cysteine.<sup>S2</sup> Then, 50  $\mu\text{L}$  of Ellman's reagent ( $4 \text{ mg mL}^{-1}$ ) was added to colorimetrically measure the chloropicrin concentration by the UV-vis spectrophotometer at the maximum adsorption wavelength ( $\lambda_{max} = 412$  nm), which is negatively correlated to the color intensity that generated from the reaction between Ellman's reagent and cysteine (Fig. S15d).

### **Paper-based colorimetric detection procedures**

The colorimetric sensing solution was prepared by dissolving NBP (20 wt%) in DMF. Then, 100  $\mu\text{L}$  of the sensing solution was dropped on a glass microfiber filter paper (diameter = 1 cm) for detection of MeI concentration in a gas chamber. The color of the sensor was read by a software of *ColorAssist* in a smart phone, and the color change after MeI detection was calculated according to Equation S1. The color difference was correlated to the concentration of MeI in the gas chamber (Fig. S14).

$$\text{Color difference} = \sqrt{(R_1 - R_0)^2 + (G_1 - G_0)^2 + (B_1 - B_0)^2} \quad (\text{S1})$$

Where  $R$ ,  $G$ , and  $B$  are the values of red, green, and blue channels of RGB color system, respectively. The subscripts of  $0$  and  $1$  refer to the samples before and after the MeI detection, respectively.

## Supplementary discussion

### Time-dependent synthesis of SAFE-Cotton

Structurally speaking, as presented in Fig. S1a, the characteristic peaks of CCl and melamine appeared in the spectrum of material obtained after 2-hours reaction. However, a sharp peak at  $850\text{ cm}^{-1}$  disappeared, referring to the consumption of triazine chlorides in CCl. Moreover, comparing with the spectrum of melamine, peaks at  $3100\text{--}3600\text{ cm}^{-1}$  shifted to lower wavenumbers, illustrating the interaction (e.g., aggregation) between CCl and melamine and mostly related to the changes of the primary amines in melamine. The FTIR spectra started to change significantly once the reaction time reached 6 hours, and no obvious difference was found by prolonging the reaction time (e.g., 24 or 48 hours). The peak change is mostly related to the disappearance of the characteristic peaks of primary amines ( $3394\text{ cm}^{-1}$ ,  $2697\text{--}2541\text{ cm}^{-1}$ ,  $1736\text{ cm}^{-1}$ , and  $1662\text{ cm}^{-1}$ ),<sup>S3</sup> which demonstrated the occurrence of the condensation reaction between melamine and CCl. More importantly, once the reaction time reached 6 hours, the characteristic peaks of triazine ring (i.e., the stretching and bending of C=N and C-N bonds) merged and became broader ( $1549\text{--}1552\text{ cm}^{-1}$ ,  $1474\text{--}1479\text{ cm}^{-1}$ ,  $1352\text{--}1354\text{ cm}^{-1}$ ).<sup>S4</sup> A sharp peak at  $813\text{ cm}^{-1}$ , which corresponds to the breathing mode of the triazine ring in the Nu-POP structure, can be observed in the spectra of the products synthesized with longer reaction times ( $> 6$  hours).

The morphology of the Nu-POP on cotton fibers is distinguishable according to synthesis time (Fig. S1b): 1) CCl and melamine form large aggregates on the fiber surface (2-hours reaction); 2) nanosized and molecular-sized aggregates covered on the fiber surfaces (6-hours reaction); 3) construction and achievement of uniform particles with mesopores on the fiber surfaces ( $>24$  hours reaction). It is important to note that both Nu-POP and SAFE-Cotton can only perform fumigant removal efficacy when the mesoporous structures are achieved. The increase of the Nu-POP

content on the SAFE-Cotton is observed when the synthesis time increased from 6 hours to 24 hours, and no further changes were noticed in the 48-hours sample. This phenomenon is consistent with the FTIR spectra as the peak intensities of the Nu-POP is relatively low when the synthesis time was only 6 hours. However, the 48-hours synthesis could result in over-oxidation and severe mechanical strength loss of the resultant SAFE-Cotton.

## **Characterization of Nu-POP after MeI adsorption and detoxification**

### ***Experimental analysis***

A serial of tests was performed to gain an insight view into the physical characteristic changes of the Nu-POP after MeI adsorption and storage detoxification (Me-Nu-POP). As shown in Fig. S10a, the N<sub>2</sub> adsorption-desorption isotherm of Me-Nu-POP showcased the type IV adsorption with a hysteresis under high partial pressure ( $P/P_0 = 0.4-1.0$ ). Compared with the brand-new Nu-POP (Fig. S2a), its BET surface area decreased to 410.22 m<sup>2</sup> g<sup>-1</sup>. Meanwhile, as presented in Fig. S10b, the pore diameter distribution did not change significantly, while a loss of the pore volume from 0.740 cm<sup>3</sup> g<sup>-1</sup> to 0.536 cm<sup>3</sup> g<sup>-1</sup> was measured. In addition, the PXRD of the Me-Nu-POP was further examined, shown in Fig. S10c. The broad peak at  $2\theta = 20^\circ$  shifted to around  $25^\circ$ , representing a change of the molecular arrangement after the alkylation of the Nu-POP by MeI. The porosity decrease of the Me-Nu-POP was expressed by the 44.0% decrease of the water regain of alkylated-Nu-POP (420.28%) to that of the Nu-POP (750.67%). Interestingly, this phenomenon is highly correlated to the MeI removal property of the alkylated-Nu-POP, whose efficiency dropped by 52.2% compared with the virgin Nu-POP (Fig. S7). This phenomenon further indicates that the fumigant removal by the Nu-POP relies more on its mesopores, where fumigant molecules can be sequestered.

### ***Computational analysis***

Density functional theory was applied to simulate the structure change of the Nu-POP before and after MeI adsorption and detoxification. As presented in Fig. S11, the geometry optimization of the Nu-POP analog with three repeating rings and its alkylated products were performed by using the Gaussian 09 program under the B3LYP/3-61G (d,p) level of theory in vacuum condition. The Nu-POP shows a planar geometry, allowing the pile-up and alignment of the polymer, which achieved the high specific surface area and massive porosity. However, the alkylation of the Nu-POP by MeI or other fumigants disordered the planarity of the Nu-POP by showing a bended geometry. The bending is caused by the steric hindrance brought from the replacement of the lone pair electrons on triazine-N to a methyl group from MeI. The disturbance of the planar geometry had been enhanced when more alkylation reactions have happened (Fig. S11). The loss of the planarity of the alkylated Nu-POP could suppress the molecular alignment, resulting in the decrease of specific surface area as well as the porosity of the alkylated Nu-POP.



### Supplementary references

S1 H. A. Patel, F. Karadas, A. Canlier, J. Park, E. Deniz, Y. Jung, M. Atilhan and C. T. Yavuz, *J. Mater. Chem.*, 2012, **22**, 8431–8437.

S2 P. Tang, H. T. Leung, M. T. Gomez and G. Sun, *ACS Sensors*, 2018, **3**, 858–866.

S3 V. Sangeetha, N. Kanagathara, R. Sumathi, N. Sivakumar and G. Anbalagan, *J. Mater.*, 2013, **2013**, 1–7.

S4 R. Xue, H. Guo, T. Wang, X. Wang, J. Ai, L. Yue, Y. Wei and W. Yang, *Mater. Lett.*, 2017, **209**, 171–174.

## Supplementary figures

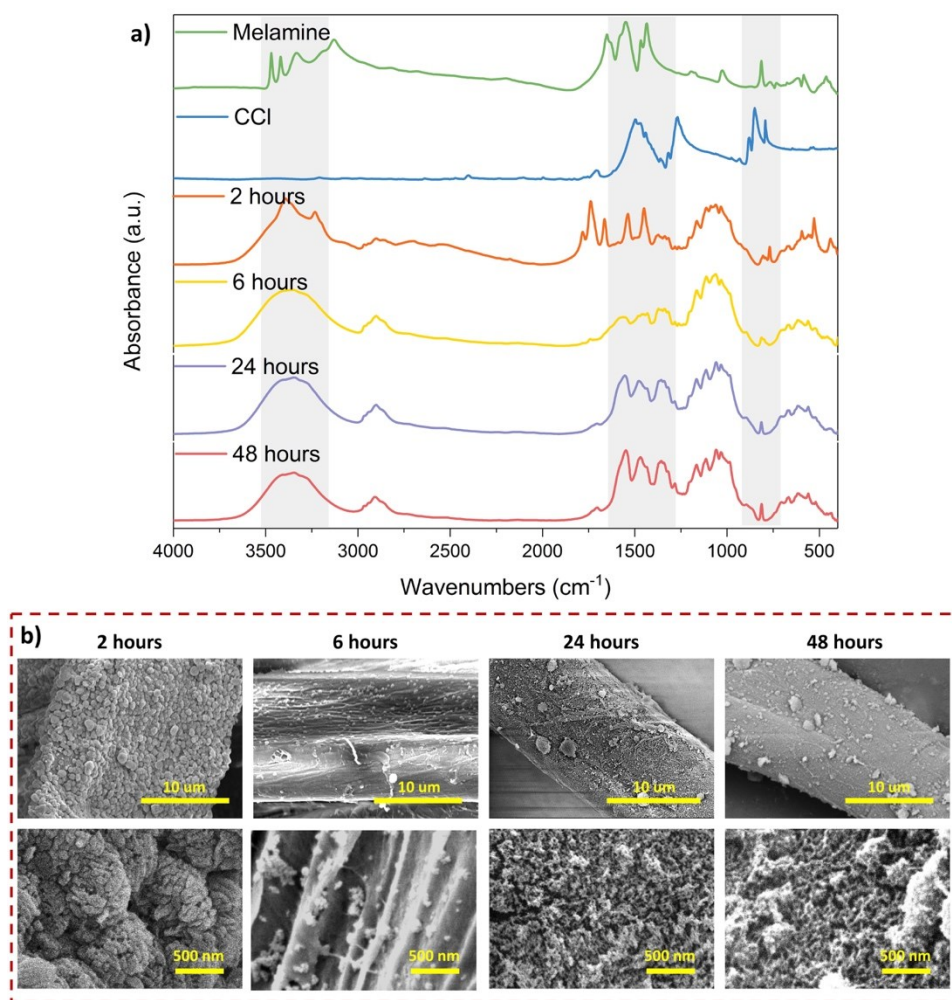


**Fig. S1** a) FTIR spectra and b) SEM images of SAFE-Cotton after different durations of *in-situ* syntheses.

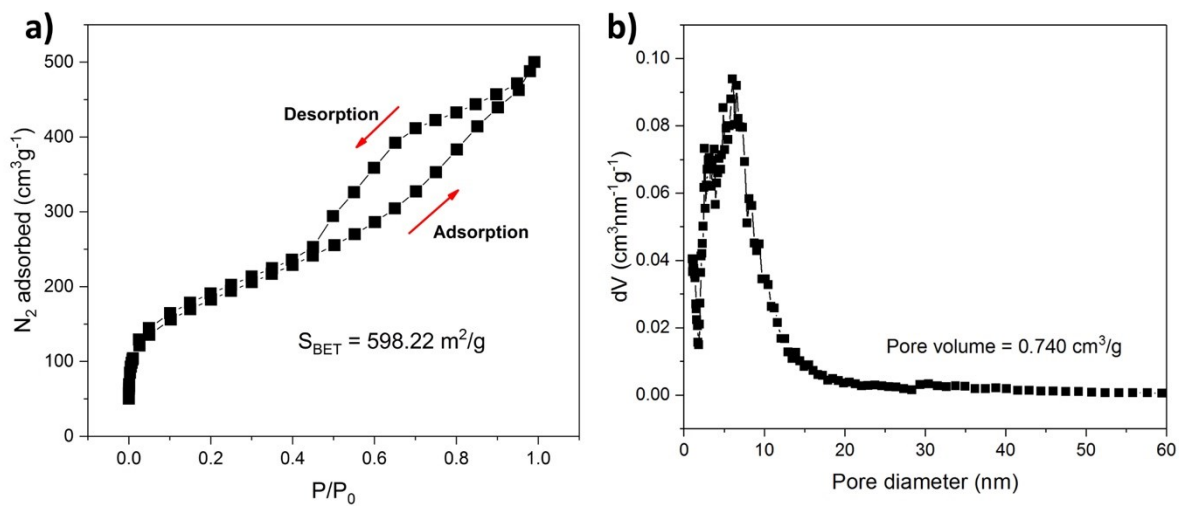


**Fig. S2** a)  $N_2$  adsorption/desorption isotherms of Nu-POP particles performed at 77 K. The BET surface area ( $S_{BET}$ ) was calculated from the  $N_2$  adsorption isotherm at 77 K. b) Pore size distribution of Nu-POP particles from 0 to 60 nm.

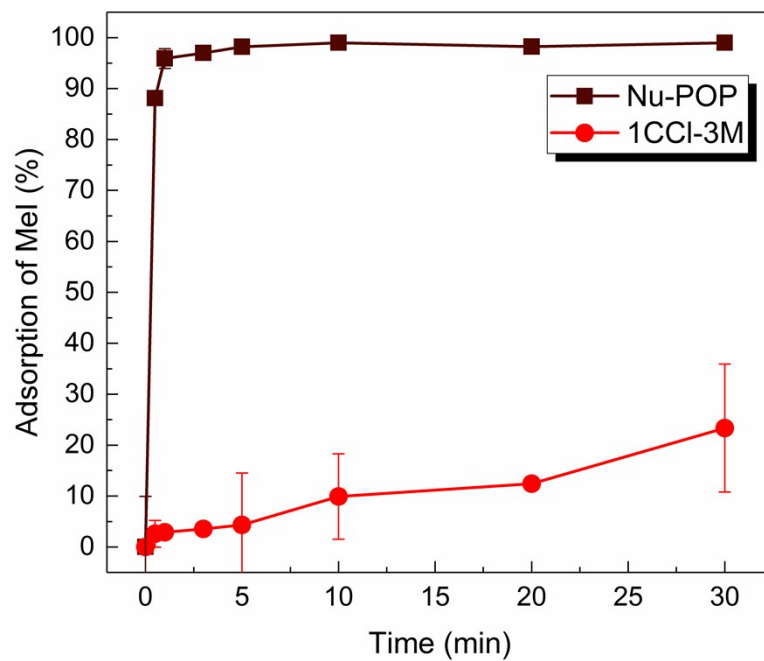


**Fig. S3** Results of MeI ( $456 \mu\text{g mL}^{-1}$ ;  $98\% \times 1 \mu\text{L}$ ) removal by Nu-POP particles and 1CCI-3M particles.

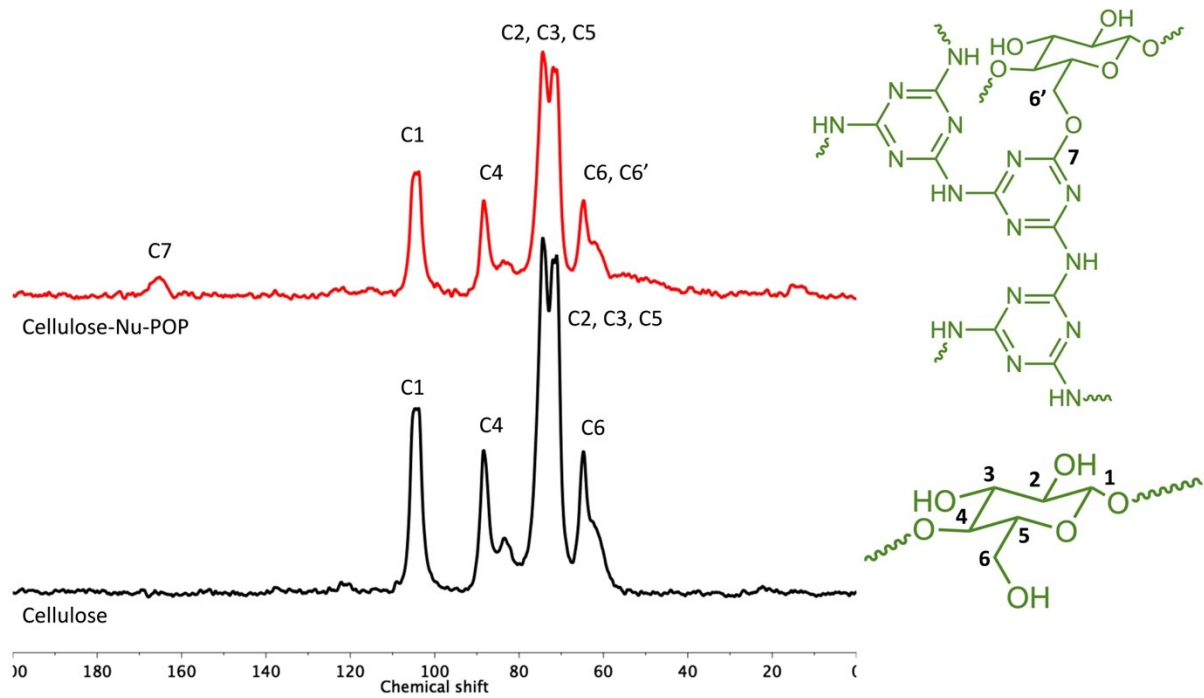


**Fig. S4** Solid state  $^{13}\text{C}$  CP/MAS NMR of SAFE-Cotton and cotton.

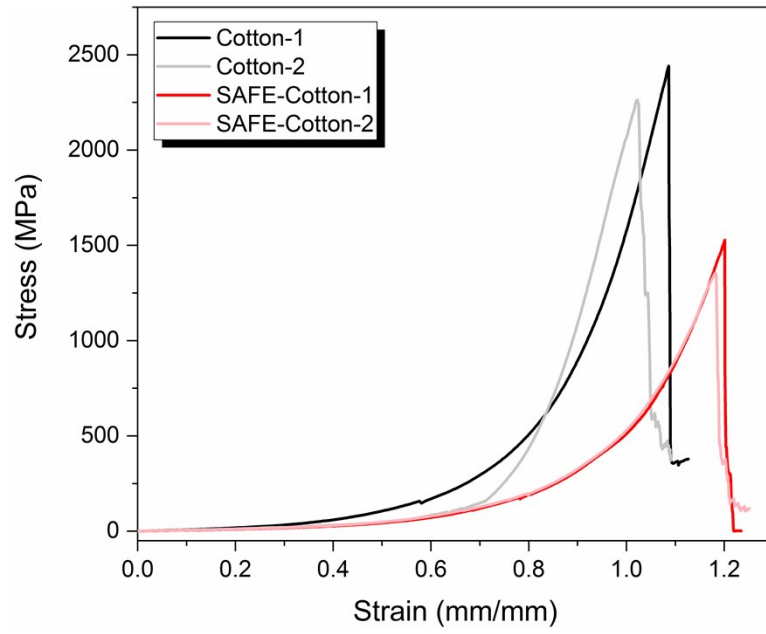


**Fig. S5** The stress-strain curve of cotton and SAFE-Cotton.

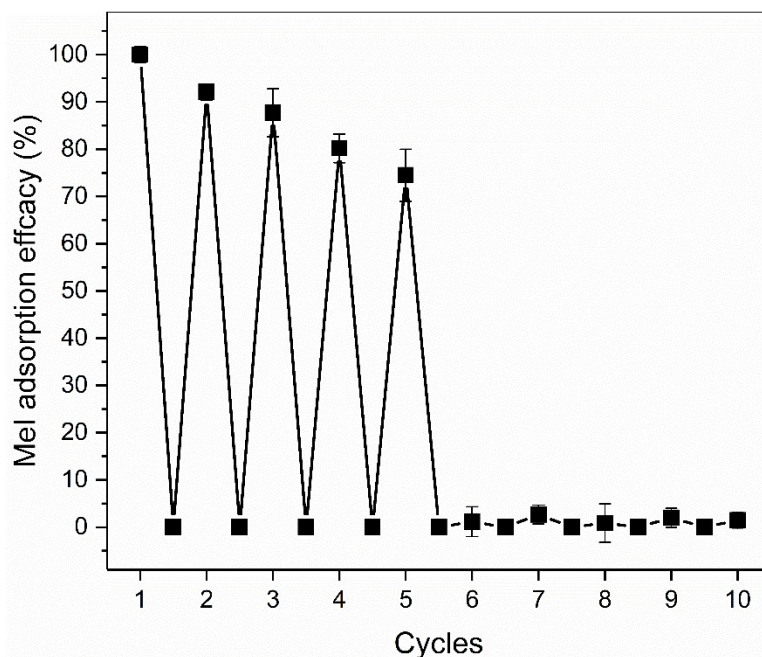


**Fig. S6** Fumigant adsorption efficiency of SAFE-Cotton with repeated challenges by MeI ( $456 \mu\text{g mL}^{-1}$ :  $98\% \times 1 \mu\text{L}$ ) without regeneration. The MeI adsorption time was 5 min in each cycle.

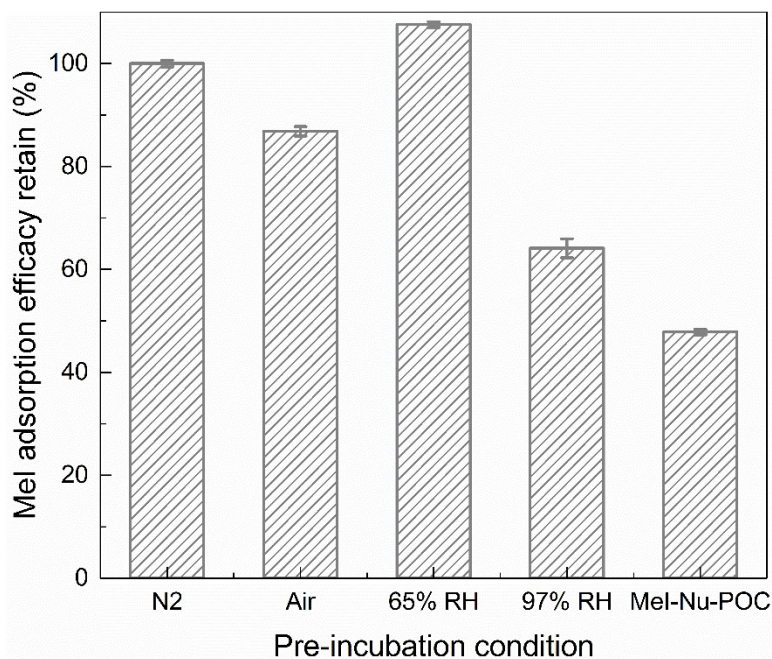


**Fig. S7** MeI adsorption efficacy recovery of SAFE-Cotton that has been pre-incubated under N<sub>2</sub>, air, and moisture conditions for 24 hours. The label of MeI-Nu-POP means the sample was pre-treated by 6840 μg mL<sup>-1</sup> of MeI (98% × 15 μL) and stored for 24 hours before testing.



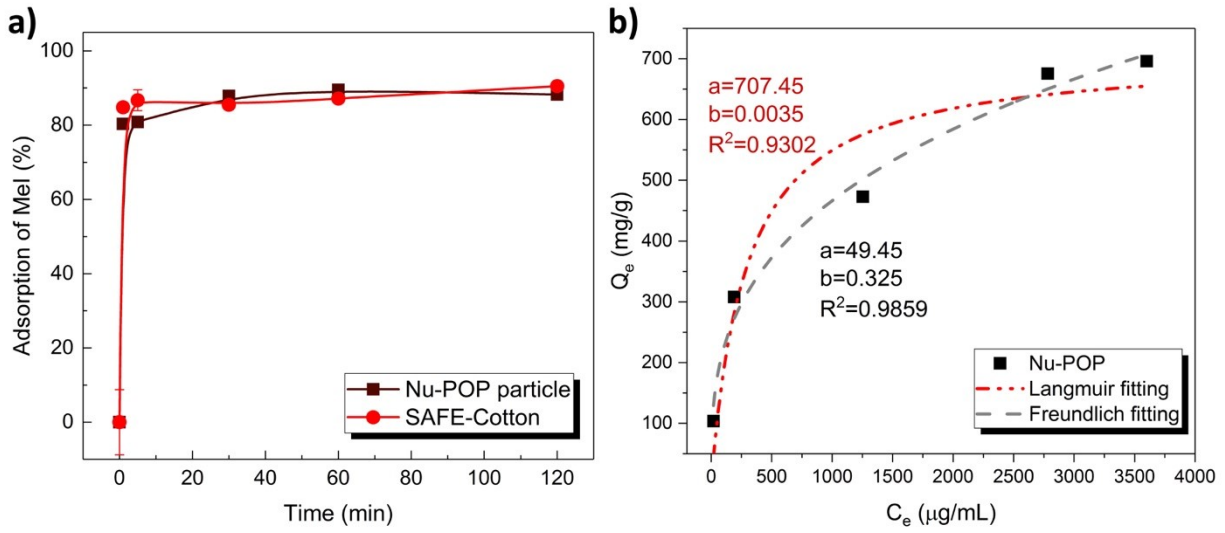


**Fig. S8** a) High amounts of MeI ( $2280 \mu\text{g mL}^{-1}$ :  $98\% \text{ MeI} \times 5 \mu\text{L}$ ) adsorption by Nu-POP particles and SAFE-Cotton according to adsorption time. b) Adsorption capacity of Nu-POP particles.

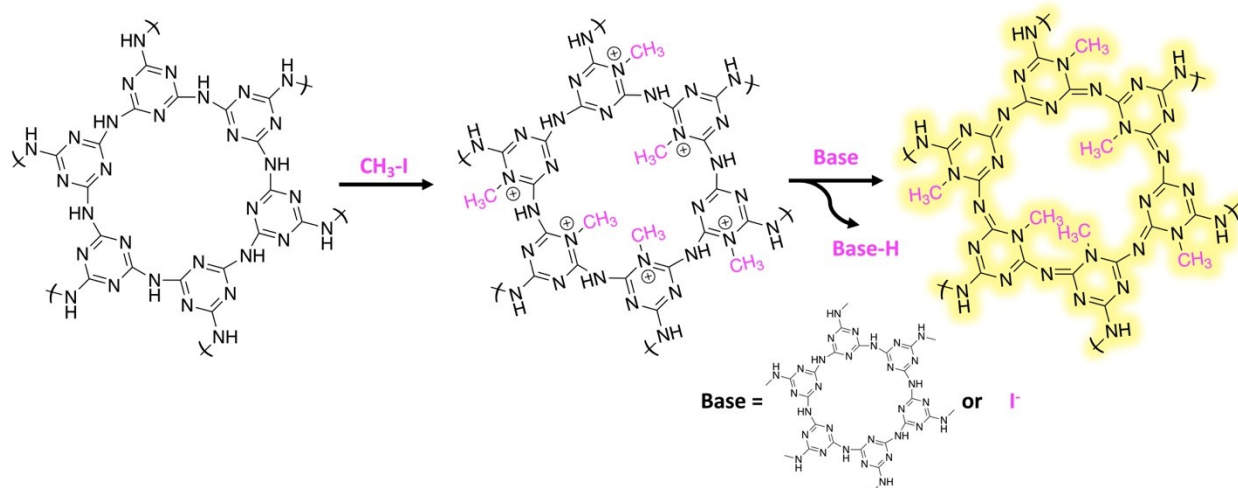


**Fig. S9** Reaction mechanism between Nu-POP and MeI, resulting in MeI detoxification and Nu-POP color change.

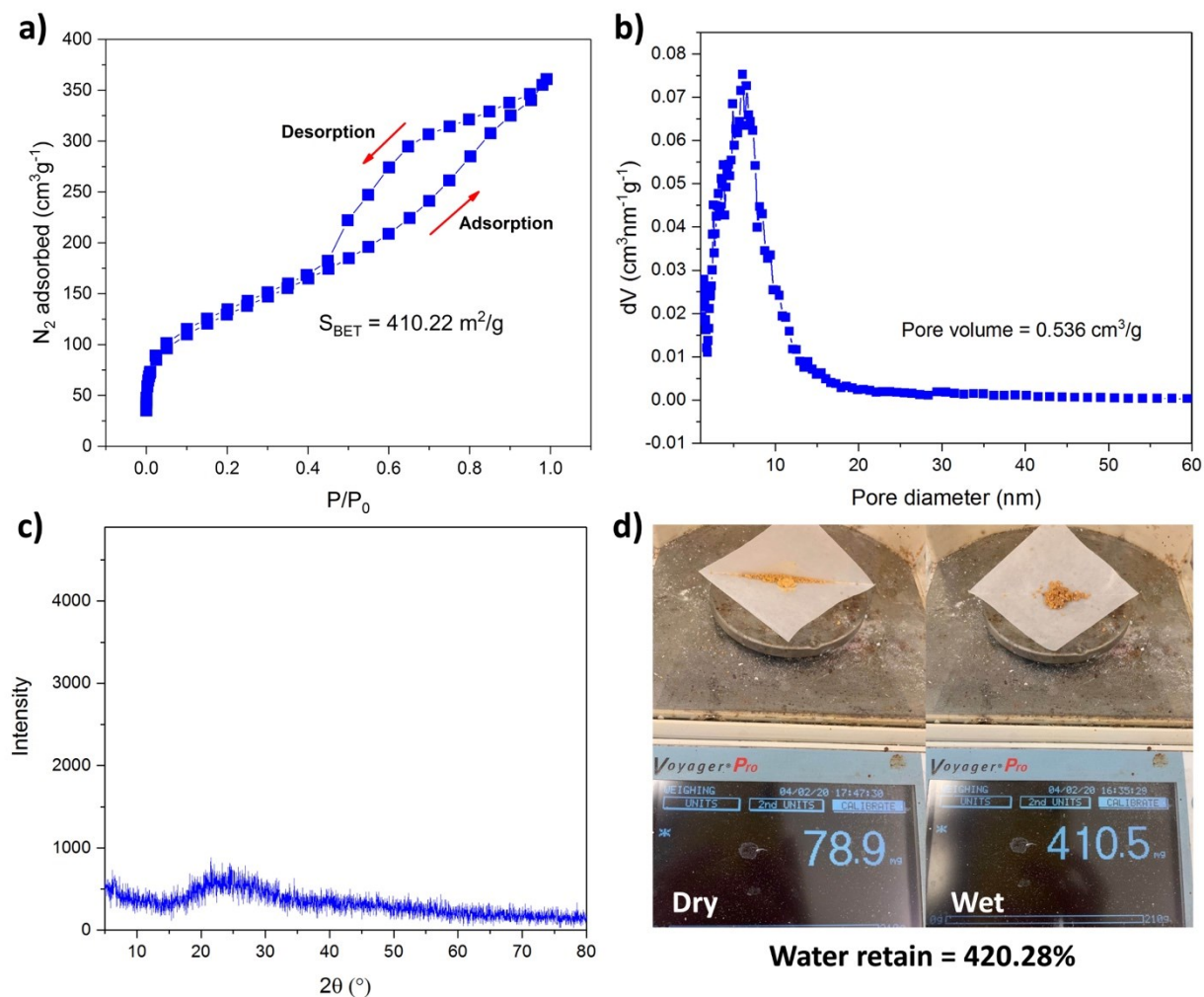


**Fig. S10** Physical characteristics of alkylated Nu-POP particles after MeI (6840  $\mu\text{g mL}^{-1}$ : 98% MeI  $\times$  15  $\mu\text{L}$ ) adsorption and detoxification (24 hours): a) N<sub>2</sub> adsorption/desorption isotherms at 77K. The  $S_{BET}$  was calculated according to the N<sub>2</sub> adsorption isotherm at 77 K. b) Pore diameter distribution. c) PXRD results. d) Optical images of dried and water-saturated particles.

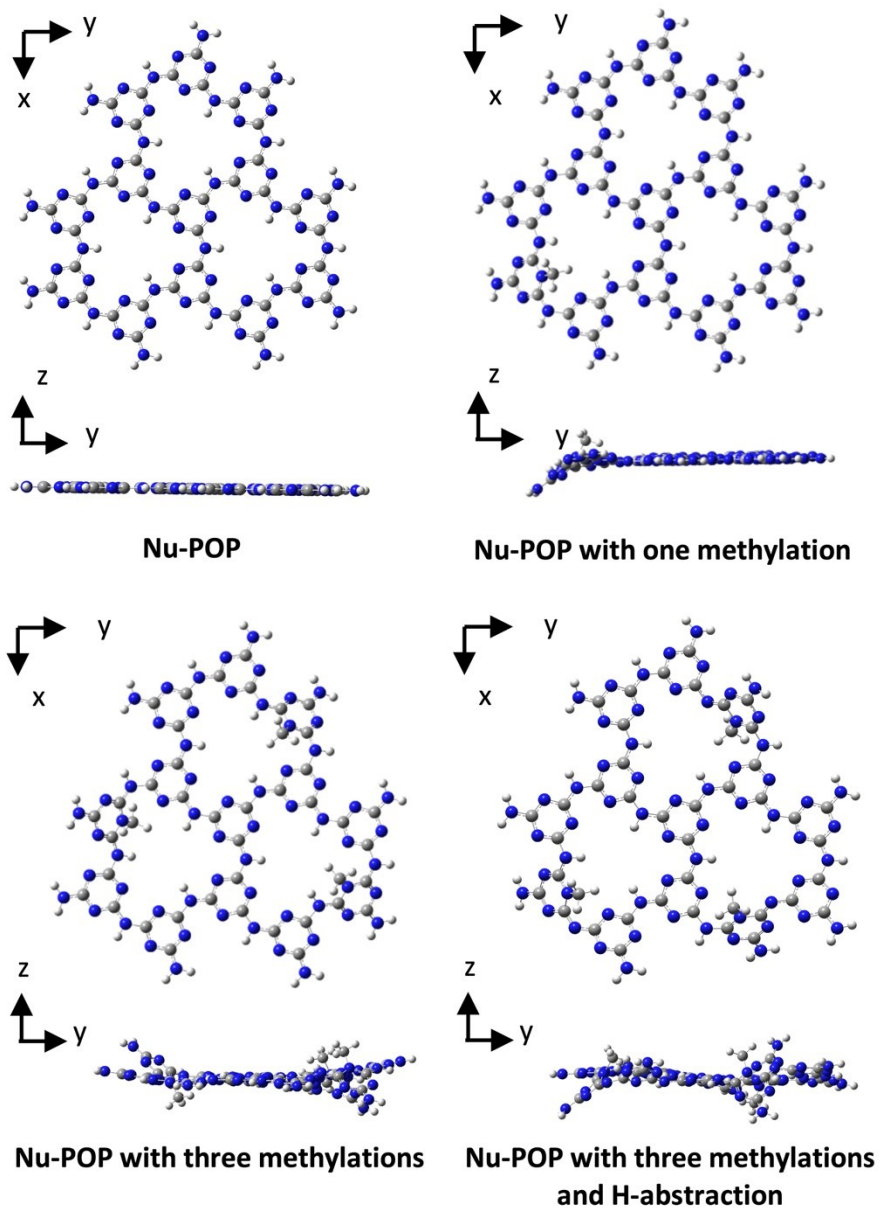


**Fig. S11** Gaussian optimized structures of Nu-POP, alkylated Nu-POP analogs.

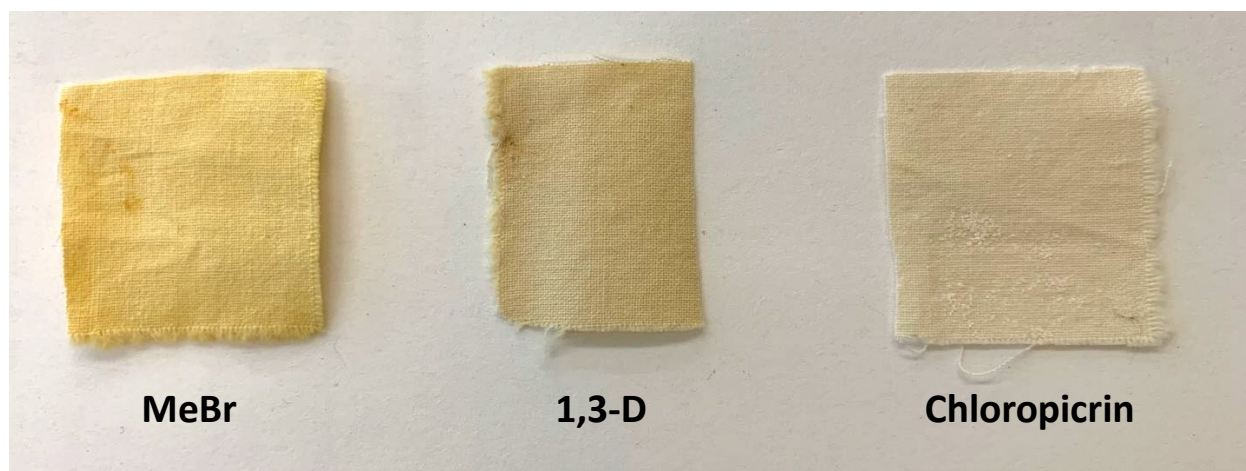


**Fig. S12** Optical images of SAFE-Cotton after adsorption and detoxification of a) MeBr, b) 1,3-D, and c) chloropicrin. The different color intensity is highly related to the degree of the detoxification reaction that had happened, which determines the residual protective functions of the used SAFE-Cotton.

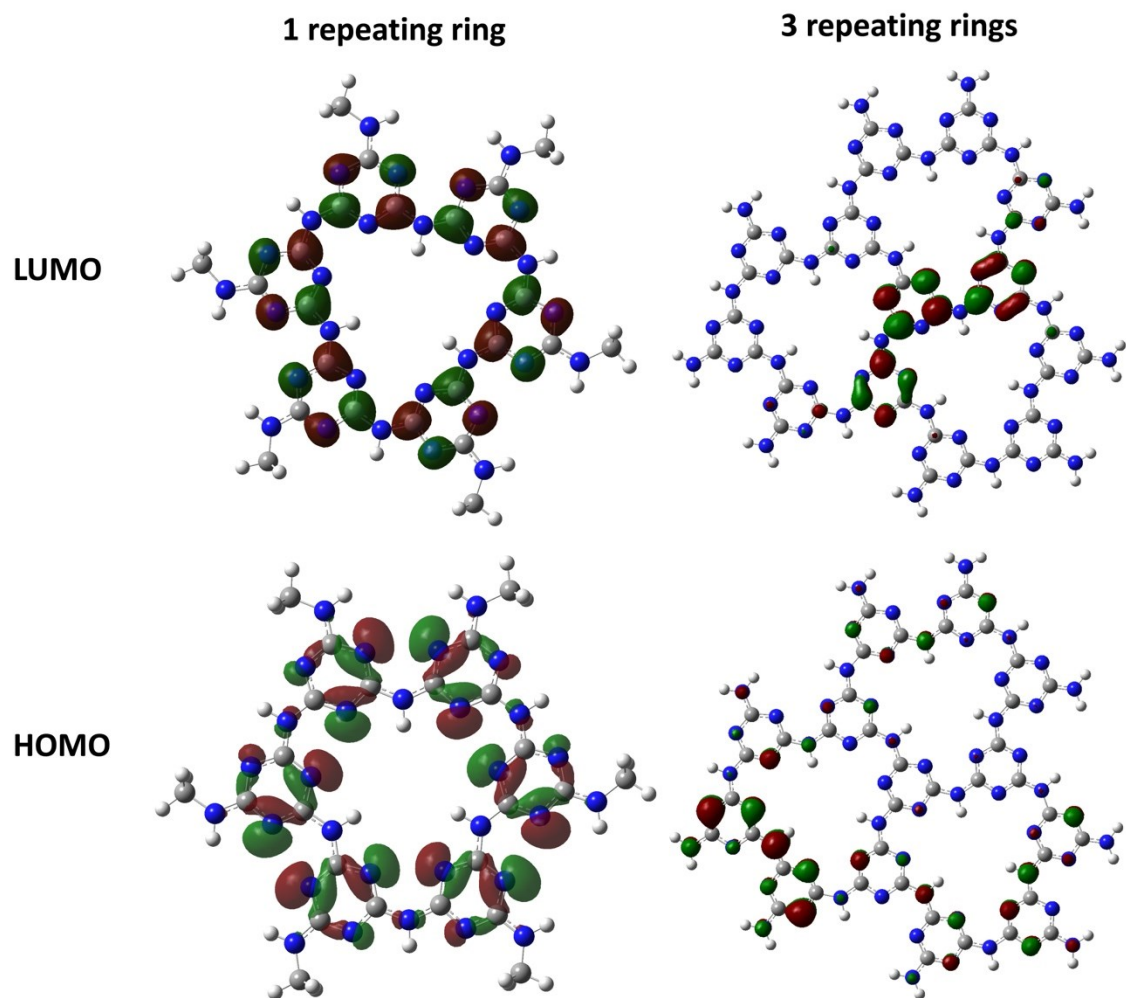


**Fig. S13** The highest occupied molecular orbital (HOMO) and the lowest unoccupied molecular orbital (LUMO) of Nu-POP analog calculated based on density functional theory. The contribution of the lone pair electrons on the triazine-N to the HOMO of the Nu-POP analog indicates the potential reactivity of the triazine-N in detoxification of alkylating fumigants as a nucleophile.

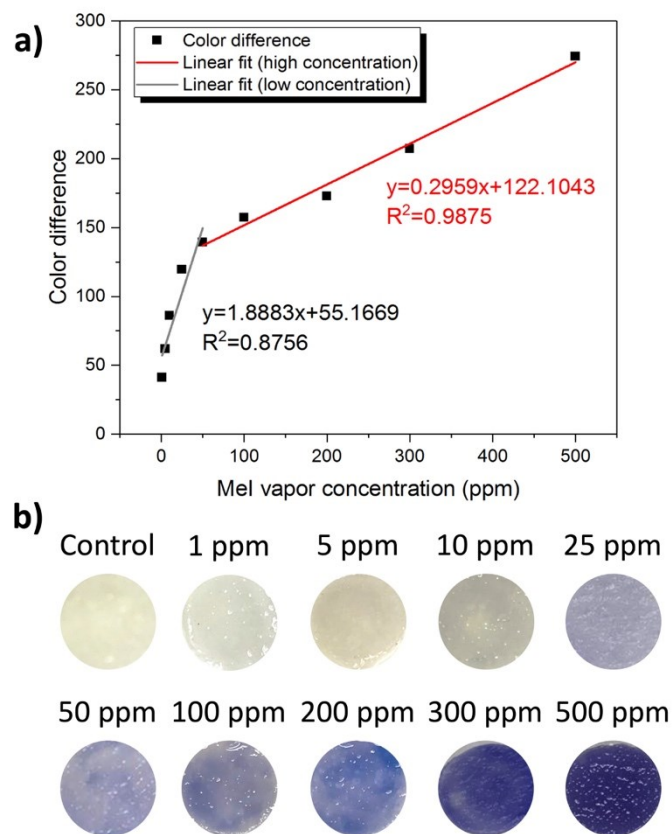


**Fig. S14** a) The calibration curve for quantification of MeI concentration according to color intensity (i.e., color difference). b) The optical images of paper-based colorimetric sensor after detecting corresponding concentration of MeI.



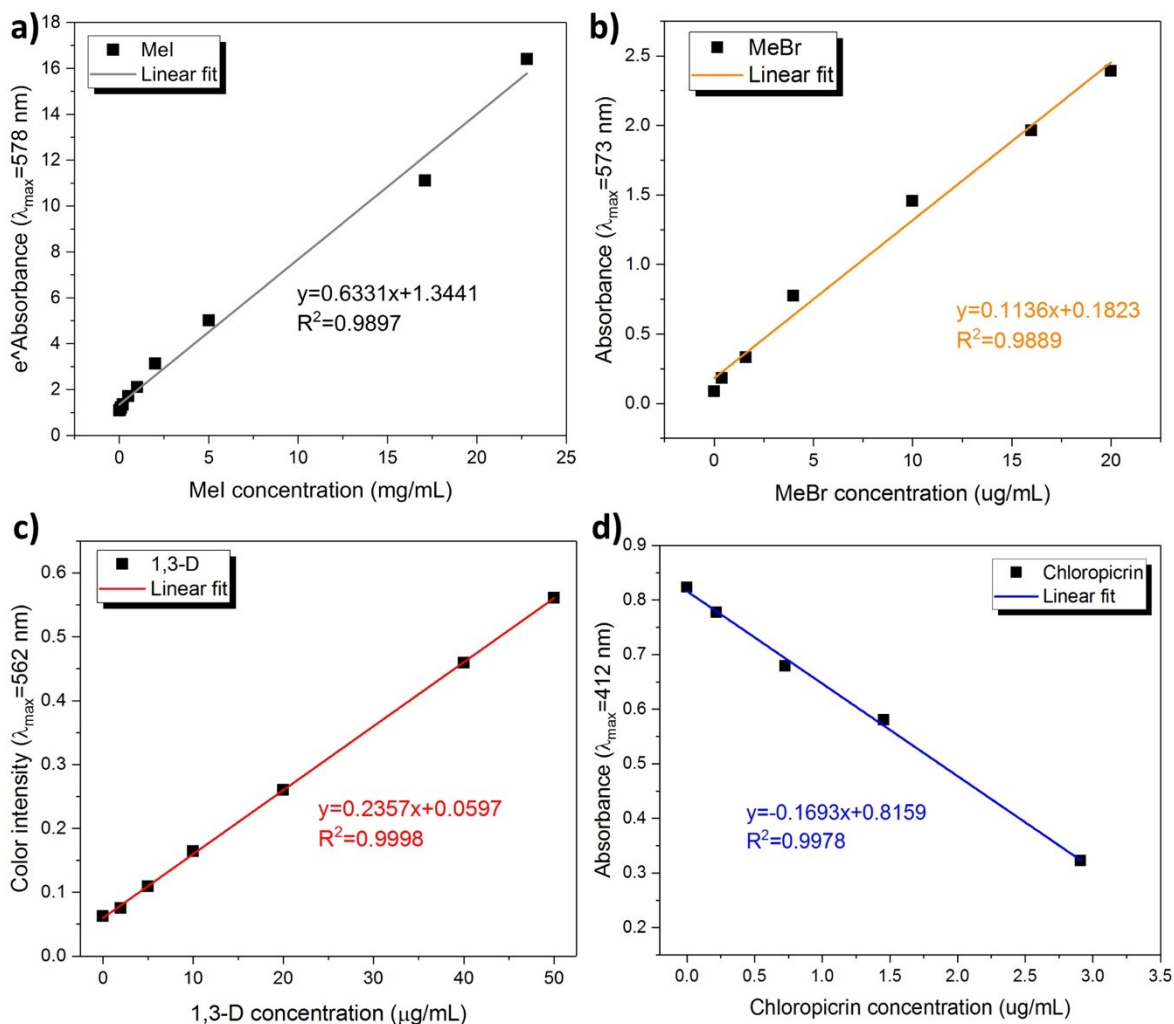
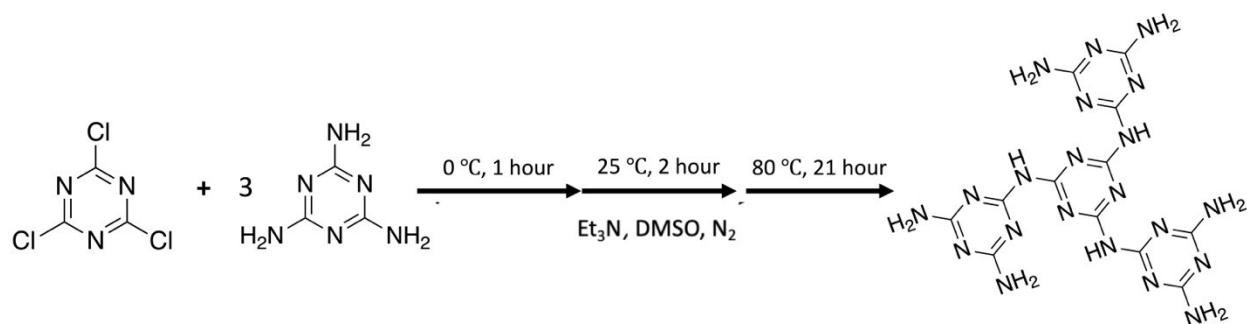


**Fig. S15** Calibration curves of the color intensity correlated to different concentration of fumigants: a) MeI, b) MeBr, c) 1,3-D, and d) chloropicrin. Here, the unit of fumigant concentration in the x-axial refers to the amount of fumigant to the volume of NBP/DMF testing solution (1 mL).



## Supplemental Scheme



**Scheme S1.** Synthesis of non-porous 1CCl-3M from CCl and melamine.

## Supplemental Table

**Table S1.** Physical properties of Nu-POP reported in literatures

Reference	BET surface area (m <sup>2</sup> g <sup>-1</sup> ) <sup>a</sup>	Pore volume (m <sup>3</sup> g <sup>-1</sup> )	Pore diameter (nm)
(23)	93.2	N/A	N/A
(24)	301.1	0.668 <sup>b</sup>	1.41 <sup>b</sup>
<b>This work</b>	598.2	0.740 <sup>a</sup>	6.079 <sup>a</sup>

a. Experimental data

b. Calculated values based on DFT theory